Received 28 January 2019; revised 30 March 2019; accepted 5 April 2019. Date of publication 11 April 2019; date of current version 26 April 2019.
The review of this paper was arranged by Editor C.-M. Zetterling.

Digital Object Identifier 10.1109/JEDS.2019.2910077

Modeling of Al Doping During 4H-SiC Chemical-Vapor-Deposition Trench Filling

KAZUHIRO MOCHIZUKI [1,2] (Senior Member, IEEE), RYOJI KOSUGI [1], YOSHIYUKI YONEZAWA [1], AND HAJIME OKUMURA [1]

1 Advanced Power Electronics Research Center, National Institute of Advanced Industrial Science and Technology, Tsukuba 305-8568, Japan
2 Center for Technology Innovation-Electronics, Hitachi, Ltd., Tokyo 185-8601, Japan

CORRESPONDING AUTHOR: K. MOCHIZUKI (e-mail: kazuhiro.mochizuki.fb@hitachi.com)

This work was supported by the Council for Science, Technology and Innovation, Cross-Ministerial Strategic Innovation Promotion Program, "Next-Generation Power Electronics/Consistent Research and Development of Next-Generation SiC Power Electronics" (funding agency: NEDO).

ABSTRACT Aluminum doping during 4H-SiC chemical-vapor-deposition (CVD) trench filling was numerically modeled toward precise design of high-voltage superjunction devices. As a first-order approximation, growth-rate- and surface-normal-scaling functions were determined based on the reported experimental results. Simulated isoconcentration contours of aluminum were confirmed to qualitatively agree with the reported imaging of doping in SiC by scanning spreading resistance microscopy. Improvement of the proposed models based on additional experiments should contribute to reducing the development time for 4H-SiC superjunction devices fabricated using CVD trench filling.

INDEX TERMS Aluminum, power semiconductor devices, silicon compounds, simulation.

I. INTRODUCTION

Superjunction (SJ) devices, in which alternating p- and n-type columns are located in a drift layer [1], [2], have been developed to improve the tradeoff relationship between breakdown voltage (*BV*) and specific on-resistance in unipolar devices. In the case of 4H-SiC SJ devices, ion implantation has been used to demonstrate *BV* of 0.8 to 2.4 kV [3]–[9]; however, chemical-vapor-deposition (CVD) trench filling, whose growth window was empirically obtained [10], should become the key technique for higher-*BV* 4H-SiC SJ devices. Although development time for such trench-filling SJ devices is expected to be reduced by using technology computer-aided design (TCAD), topography simulation [11], [12], a part of TCAD, has not been widely used due to its inability to simulate a distribution of acceptor concentration (N_A) in filled trenches. Instead, only device simulation was carried out by assuming a fixed N_A in the filled trenches [13]–[19] or two different values of N_A in the regions close to the trench sidewalls and in the rest of the filled trenches [20].

In-situ p-type doping in 4H-SiC CVD is usually carried out by the addition of trimethylaluminum. The efficiency of aluminum incorporation into solid SiC needs to be represented in topography simulation by a scaling function k, which is, in general, influenced by the strain [21] and surface orientation effects [22]. The radius of an aluminum ion having the coordination number of four (i.e., 0.039 nm [23]) is about twice as large as the average of the radii of silicon and carbon ions having the coordination number of four {i.e., $(0.026 + 0.015)/2 = 0.021$ nm [23]}. An aluminum atom once incorporated into the solid thus tends to be pushed out into vapor; however, when the growth rate normal to the growing surface (R_g) is too high, it does not have enough time to escape from the solid (i.e., $k = 1$). In contrast, N_A decreases to its equilibrium value when R_g is close to zero [24]. Such R_g-dependent N_A was experimentally observed by Forsberg *et al.* with respect to growth on 4H-SiC (0001) substrates [25]. Negoro *et al.*, on the other hand, reported an influence of $\{1\bar{1}00\}$ faces (whose normal vector has an angle θ of 90° from the [0001] direction) on N_A [26]. Although the trenches were filled with Al-doped SiC, the regions close to $\{1\bar{1}00\}$ trench sidewalls became n-type when the carbon-to-silicon ratio in the input gas (*C/Si*) was unity. Since the regions became p-type in the case $C/Si \geq 2$ [26], the surface orientation dependence of k is considered to be a function of θ and *C/Si*.

Judging from these reports [25], [26], we must set our final goal to determine $k(R_g, \theta, C/Si)$ contours for practical topography simulation. Because of the limited experimental results, however, only a growth-rate-scaling function $k(R_g)$ or a surface-normal-scaling function $k(\theta)$ was used in this paper as a first order approximation.

II. SIMULATION MODELS

The surface reactions during 4H-SiC CVD based on SiH_4 and C_3H_8 [(a) and (a') in Fig. 1] are known to be so fast [27] that trench filling is limited by either vapor-phase diffusion (in the case of growth on a rough surface) [(b) in Fig. 1] or surface diffusion (in the case of growth on a step-and-terrace surface) [(c) in Fig. 1] of growing species. As an example of the former case, a scanning spreading resistance microscopy (SSRM) image of doping in a 7-μm-deep trench [20] is shown in Fig. 2. There seem to be no facets appeared on the grown surface, indicating the trench was filled in the growth mode on a rough surface. High resistivity (namely, low N_A) regions exist along the trench sidewalls, and the resultant boundaries between the low N_A regions and the center region with high N_A are almost vertical.

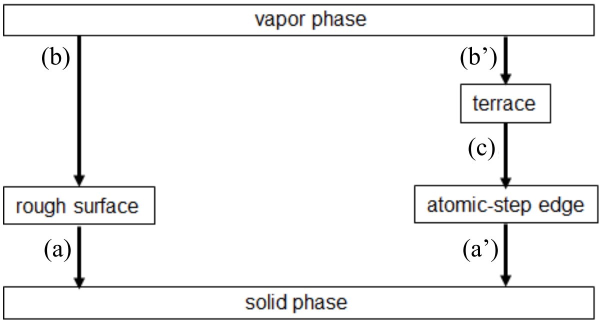

FIGURE 1. Flow chart of epitaxial growth processes. (a)(a') Surface reactions. (b)(b') Vapor-phase diffusion. (c) Surface diffusion.

As shown schematically in Fig. 3, on the other hand, Malhan *et al.* reported that the low N_A regions (B1 and B2) are sandwiched between the high N_A regions (A/C1 and A/C2, respectively) and that the boundaries between the low and high N_A regions are inclined from the vertical direction [28]. Since faces with θ of about 45° [i.e., $\{1\bar{1}0n\}$ $(n\sim4)$] are known as facets [29], the low N_A regions (B1 and B2) in Fig. 3 are considered to be the tracks of such facets on which growing species diffused [21]. Since surface diffusion was difficult to be included in the commercial topography simulator used (Victory Process 2D [30]), this study covers growth on a rough surface (Fig. 2) only.

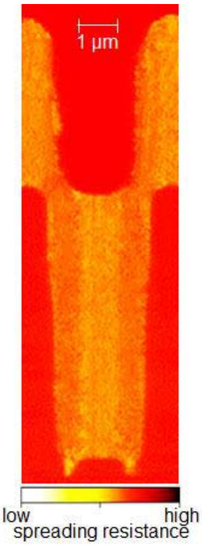

FIGURE 2. Cross-sectional SSRM image of 7-μm-deep filled trench, as seen as the $[11\bar{2}0]$ direction, reported in [20].

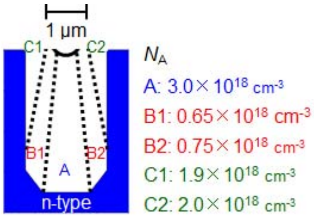

FIGURE 3. Schematic cross-sectional SSRM image of 3.5-μm-deep filled trench, as seen as the $[11\bar{2}0]$ direction, reported in [28]. Due to the difficulty in clearly reproducing the reported SSRM image, we just traced the boundaries that were drawn in [28].

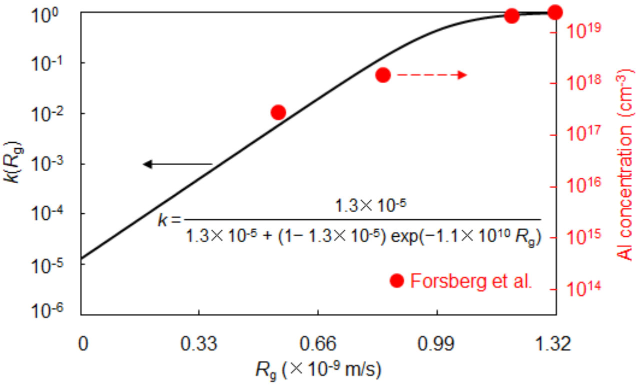

FIGURE 4. Measured aluminum concentration (shown in the right-hand vertical axis) as a function of R_g [25] and modeled growth-rate-scaling function (shown in the left-hand vertical axis).

A. MODEL FOR A GROWTH-RATE-SCALING FUNCTION

The solid circles in Fig. 4 show the reported aluminum concentration in 4H-SiC grown on (0001) substrates at surface temperature T of 1873 K [25]. With respect to surface roughness during CVD trench filling of 4H-SiC, the present authors experimentally showed that the surface on the mesa top was rough in the case $T \geq 1843$ K, while it was smooth in the case $T \leq 1823$ K [31]. We therefore considered the experimental data in Fig. 4 represent N_A in 4H-SiC grown on a rough surface and modeled $k(R_g)$ by vertically displacing the data, as shown by the solid line. In reference to the Burton-Prim-Slichter theory, which was

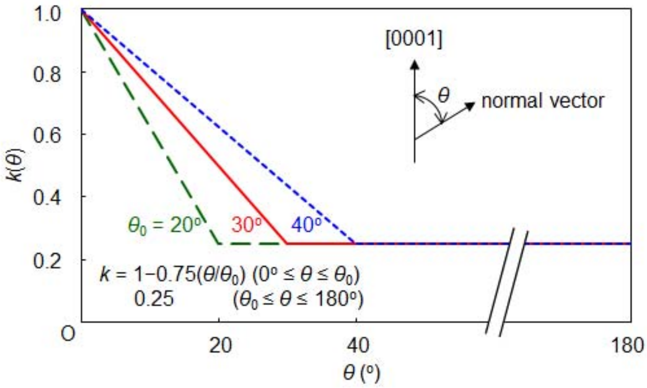

FIGURE 5. Modeled surface-normal-scaling function. Definition of θ is shown in the inset.

successfully applied to k in silicon gown from the melt [32], $k(R_g)$ was fitted as

$$k\left(R_g\right) = k^e / \left[k^e + \left(1 - k^e\right)\exp\left(-1.1 \times 10^{10}/R_g\right)\right] \text{ and} \tag{1a}$$

$$k^e = 1.3 \times 10^{-5}, \tag{1b}$$

where k^e represents $k(R_g = 0)$ under the equilibrium condition.

B. MODEL FOR A SURFACE-NORMAL-SCALING FUNCTION

The ratio of the low N_A to the high N_A in Fig. 2 was reported to be 0.25, although the values of N_A were not measured [20]. Since the *C/Si* was less than unity [20], the effect of incorporation of nitrogen donors [26] seemed to affect the measured $k(\theta = 90°)$ of 0.25. According to the experiments by Forsberg *et al.*, $k(\theta = 180°)$ was also considered to be small [25]. $k(\theta)$ was therefore fitted simply as

$$k(\theta) = 1 - 0.75(\theta/\theta_0)\left(0° \le \theta \le \theta_0\right) \text{ and} \tag{2a}$$

$$0.25(\theta_0 \le \theta \le 180°). \tag{2b}$$

Eqs. (2a) and (2b) are shown in Fig. 5 in the cases $\theta_0 = 20°$, 30°, and 40°.

III. SIMULATION

Based on the result in Fig. 2, a 7-µm-deep trench having 0.5-µm-deep subtrenches (Fig. 6) was numerically investigated. Since the conditions for the trench-filling growth were not described in detail [20], the following conditions for the boundary-layer model in topography simulation [11] were tentatively assumed:

$$C^e(\infty) = 8.775 \times 10^{-9}\text{kmol/m}^3, \tag{3a}$$

$$C^0 = 8.952 \times 10^{-9}\text{kmol/m}^3, \tag{3b}$$

$$L_L = 1.5 \text{ mm}, \tag{3c}$$

$$T = 1923 \text{ K}, \text{ and} \tag{3d}$$

$$\gamma = 0.1 \text{ J/m}^2, \tag{3e}$$

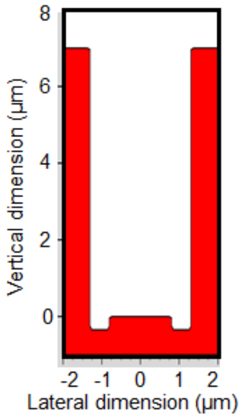

FIGURE 6. Initial structure used for topography simulation. The trench is 7 μm deep and the subtrenches are 0.5 μm deep.

where $C^e(\infty)$ and C^0 are vapor-phase concentrations of growing species in the vicinity of an infinite plane and at the top of the boundary layer, respectively, L_L is the thickness of the boundary layer, and γ is the surface free energy of 4H-SiC during growth [11]. The effective vapor-phase diffusivity of growing species (D^{eff}) was determined from the growth rate on an infinite plane (R_0), which was chosen as an input parameter.

R_g was determined from the following equations: [11]

$$\partial\varphi/\partial t + R_g(\partial\varphi/\partial x + \partial\varphi/\partial y) = 0, \tag{4}$$

$$R_g = \left[-D^{eff}\left(C|_{\text{growing surface}} - C^e(r)\right)/\partial \boldsymbol{n}\right]V_m, \text{ and} \tag{5}$$

$$C^e(r) = C^e(\infty)\exp(\gamma V_m/RTr), \tag{6}$$

where $\varphi(x, y)$ is a level-set function defined as a function of the signed distance from the point (x, y) to the growing surface, $\boldsymbol{n}$ is the vector normal to the growing surface, $C^e(r)$ is the equilibrium vapor-phase concentration of growing species in the vicinity of a growing surface with a radius of curvature r, V_m is the molar volume of 4H-SiC (1.25×10^{-5} m^3/mol) [33], and R is the ideal gas constant. Eq. (6) is known as the Gibbs–Thomson effect [34]. Eqs. (4) and (5) were solved by methods that use the high-order nonoscillatory schemes for Hamilton-Jacobi equations [35].

IV. RESULTS AND DISCUSSION

In the case that k can be assumed to be independent of θ and *C/Si*, the maximum doping level of aluminum (N_{max}), which corresponds to N_A at $k = 1$, was assumed to be 3.0×10^{17} cm^{-3} to give N_A of 2.0×10^{16} cm^{-3} that was assumed for device simulation in [20]. As shown in Fig. 7(b), the use of $R_0 = 0.90$ µm/h reproduces the result in Fig. 2 qualitatively. When R_0 is lower (i.e., 0.42 μm/h), N_A in the region around the trench bottom is too low [Fig. 7(a)]. When R_0 is higher (i.e., 1.7 μm/h), on the other hand, the width of the regions (with low N_A) close to the trench sidewalls is too narrow [Fig. 7(c)]. Figs. 8(a)-(c) shows topography changes over growth time in the case $R_0 = 0.9$ µm/h. During the initial stage of trench filling, the

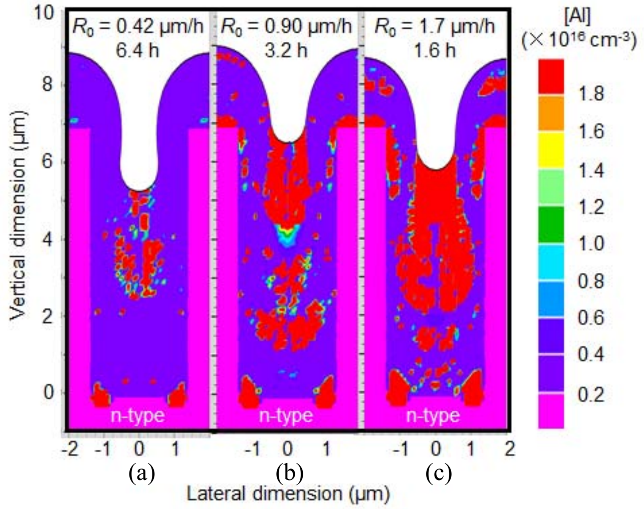

FIGURE 7. Simulated isoconcentration contours of aluminum in (a) 6.4-h ($R_0 = 0.42$ μm/h), (b) 3.2-h ($R_0 = 0.90$ μm/h), and (c) 1.6-h ($R_0 = 1.7$ μm/h) grown 4H-SiC filled trenches when k is a function of R_g only.

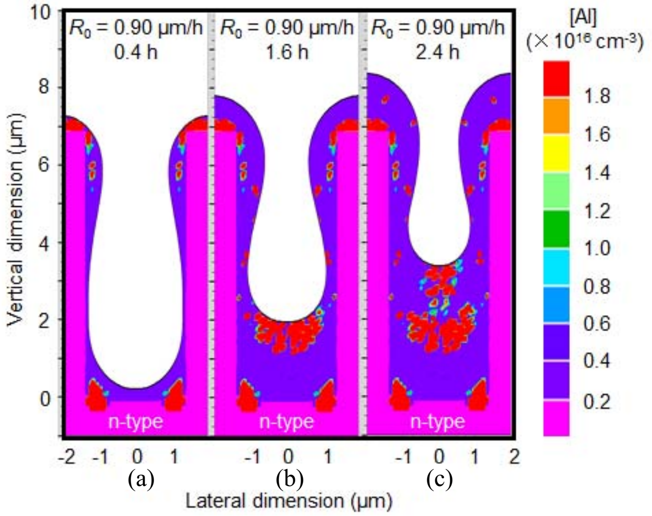

FIGURE 8. Simulated isoconcentration contours of aluminum in (a) 0.4-h, (b) 1.6-h, and (c) 2.4-h grown 4H-SiC filled trenches when R_0 is 0.90 μm/h and k is a function of R_g only.

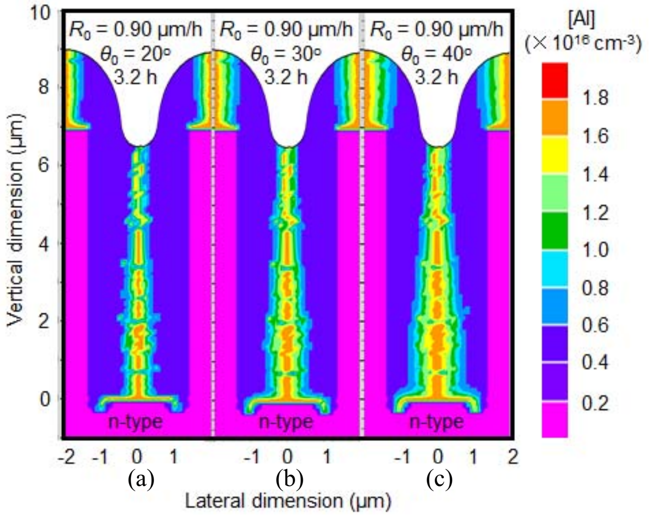

FIGURE 9. Isoconcentration contours of aluminum in 3.2-h grown trenches simulated by assuming θ_0 of (a) 20°, (b) 30°, and (c) 40° when R_0 is 0.90 μm/h and k is a function of θ only.

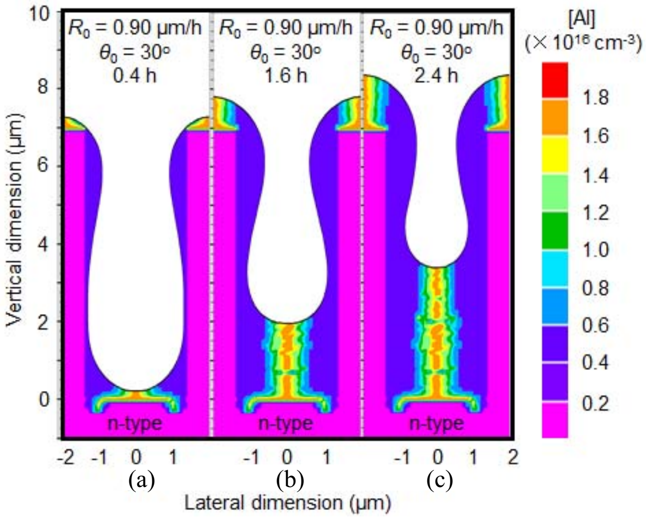

FIGURE 10. Simulated isoconcentration contours of aluminum in (a) 0.4-h, (b) 1.6-h, and (c) 2.4-h grown 4H-SiC filled trenches when R_0 is 0.90 μm/h and k is a function of θ only.

regions with $r < 0$ (in the subtrenches and around the corners of the trench bottom) are filled rapidly due to Eqs. (5) and (6), resulting in high N_A there [Fig. 8(a)]. The region with $r < 0$ then moves to the center of the trench [Fig. 8(b)]. Since the center region comes to have high R_g, it continues to have high N_A [Figs. 8(c) and 7(b)].

In contrast, the case that k can be assumed to be independent of R_g and *C/Si* is considered to correspond to the case of R_g being too high. N_{max} was therefore assumed to be 2.0×10^{16} cm^{-3}. As shown in Fig. 9(c), the use of $\theta_0 = 40°$ results in the sloped boundaries between the low and high N_A regions. In the cases $\theta_0 = 20°$ or 30°, on the other hand, the boundaries become relatively vertical [Figs. 9(a) and 9(b)], which are similar to the SSRM image in Fig. 2. However, the width of the high N_A region is narrower than that in Fig. 2. Topography changes over growth time are thus shown in Figs. 10(a)-(c) in the case $\theta_0 = 30°$ only. From the initial stage of trench filling [Fig. 10(a)], N_A becomes large both in the subtrenches and in the region on the mesa top.

The comparison between these two cases is the advantage of the latter. For further investigation, however, computational fluid dynamics simulation (based on the detailed growth conditions) and quantitative analysis of the experimental observation (Fig. 2) are needed in both models for $k(R_g)$ and $k(\theta)$. Additional experiments can also improve these functions of one variable to $k(R_g, \theta, C/Si)$ contours for practical topography simulation, which should contribute to reducing the development time for 4H-SiC SJ devices fabricated using CVD trench filling.

Note that the filled subtrenches with high N_A will lead to local electric-field concentration in reverse-biased SJ devices. To avoid that prospect, either fabricating subtrench-free trenches or making a start of trench-filling growth by a thin n-type layer should be required.

V. CONCLUSION

Aluminum doping during 4H-SiC CVD trench filling was numerically modeled. As a first order approximation, growth-rate- and surface-normal-scaling functions were determined from the reported experimental results. The resultant iso-concentration contours of aluminum were qualitatively agreed with the reported SSRM image. Improvement of the proposed models based on additional experiments should accelerate development of high-voltage 4H-SiC SJ devices.

ACKNOWLEDGMENT

K. Mochizuki thanks Professor Emeritus Tatau Nishinaga of the University of Tokyo for expounding on impurity segregation during epitaxial growth.

REFERENCES

[1] T. Fujihira, "Theory of semiconductor superjunction devices," *Jpn. J. Appl. Phys.*, vol. 36, no. 10, pp. 6254–6262, Oct. 1997.

[2] F. Udrea, G. Deboy, and T. Fujihira, "Superjunction power devices, history, development, and future prospects," *IEEE Trans. Electron Devices*, vol. 64, no. 3, pp. 720–727, Mar. 2017.

[3] R. Kosugi *et al.*, "First experimental demonstration of SiC super-junction (SJ) structure by multi-epitaxial growth method," in *Proc. Int. Symp. Power Semicond. Devices ICs*, Jun. 2014, pp. 346–349.

[4] X. Zhong, B. Wang, and K. Sheng, "Design and experimental demonstration of 1.35 kV SiC super junction Schottky diode," in *Proc. Int. Symp. Power Semicond. Devices ICs*, Prague, Czech Republic, Jun. 2016, pp. 231–234.

[5] T. Masuda, R. Kosugi, and T. Hiyoshi, "0.97 mΩcm^2/820 V 4H-SiC super-junction V-groove trench MOSFET," *Mater. Sci. Forum*, vol. 897, pp. 483–488, May 2017.

[6] R. Kosugi *et al.*, "Current status of SiC super-junction (SJ) device development," in *Proc. 4th Meeting Adv. Power Semicond.*, Nagoya, Japan, Nov. 2017, pp. 27–28.

[7] X. Zhong, B. Wang, J. Wang, and K. Sheng, "Experimental demonstration and analysis of a 1.35-kV 0.92-mΩcm^2 SiC superjunction Schottky diode," *IEEE Trans. Electron Devices*, vol. 65, no. 4, pp. 1458–1465, Apr. 2018.

[8] T. Masuda, Y. Saito, T. Kumazawa, T. Hatayama, and S. Harada, "0.63 mΩcm^2/ 1170 V 4H-SiC super junction V-groove trench MOSFET," *Tech. Dig. Int. Electron Devices Meeting*, San Francisco, CA, USA, Dec. 2018, pp. 8.1.1–8.1.4.

[9] S. Harada *et al.*, "First demonstration of dynamic characteristics for SiC superjunction MOSFET realized using multi-epitaxial growth method," *Tech. Dig. Int. Electron Devices Meeting*, San Francisco, CA, USA, Dec. 2018, pp. 8.2.1–8.2.4.

[10] S. Ji *et al.*, "An empirical growth window concerning the input ratio of HCl/SiH$_4$ gases in filling 4H-SiC trench by CVD," *Appl. Phys. Exp.*, vol. 10, no. 5, pp. 1–4, May 2017.

[11] K. Mochizuki, S. Ji, R. Kosugi, Y. Yonezawa, and H. Okumura, "First topography simulation of SiC-chemical-vapor-deposition trench filling, demonstrating the essential impact of the Gibbs-Thomson effect," *Tech. Dig. Int. Electron Devices Meeting*, San Francisco, CA, USA, Dec. 2017, pp. 35.4.1–35.4.4.

[12] K. Mochizuki, S. Ji, R. Kosugi, Y. Yonezawa, and H. Okumura, "Topography simulation of 4H-SiC-chemical-vapor-deposition trench filling including an orientation-dependent surface free energy," in *Proc. Int. Conf. Simulat. Semicond. Processes Devices*, Austin, TX, USA, Sep. 2018, pp. 331–335.

[13] K. Adachi *et al.*, "Comparison of super-junction structures in 4H-SiC and Si for high voltage applications," *Mater. Sci. Forum*, vols. 353–356, pp. 719–722, Jan. 2001.

[14] L. Zhu, P. Losee, and T. P. Chow, "Design of high voltage 4H-SiC superjunction Schottky rectifiers," *Int. J. High Speed Electron. Syst.*, vol. 14, no. 3, pp. 865–871, Sep. 2004.

[15] L. C. Yu and K. Sheng, "Breaking the theoretical limit of SiC unipolar power device—A simulation study," *Solid-State Electron.*, vol. 50, no. 6, pp. 1062–1072, Jun. 2006.

[16] L. Yu and K. Sheng, "Modeling and optimal device design for 4H-SiC super-junction devices," *IEEE Trans. Electron Devices*, vol. 55, no. 8, pp. 1961–1969, Aug. 2008.

[17] C. Lin, P. Hong-Bin, C. Zhi-Ming, and Z. Yuan, "Analysis and simulation of a 4H-SiC semi-superjunction Schottky barrier for softer reverse-recovery," *Chin. Phys. B*, vol. 21, no. 1, pp. 1–4, Jan. 2012.

[18] H. Kang and F. Udrea, "Material limit of power devices—Applied to asymmetric 2-D superjunction MOSFET," *IEEE Trans. Electron Devices*, vol. 65, no. 8, pp. 3326–3332, Aug. 2018.

[19] X. Zhou, Z. Guo, and T. P. Chow, "Performance limits of vertical 4H-SiC and 2H-GaN superjunction devices," in *Proc. Eur. Conf. SiC Related Mater.*, Birmingham, U.K., Sep. 2018, paper no. WE.P.MO7.

[20] R. Kosugi *et al.*, "Development of SiC super-junction (SJ) device by deep trench-filling epitaxial growth," *Mater. Sci. Forum*, vols. 740–742, pp. 785–788, Jan. 2013.

[21] T. Nishinaga, C. Sasaoka, and K. Pak, "Study of nitrogen inhomogeneity in LPE GaP by spatially resolved photoluminescence," *Jpn. J. Appl. Phys.*, vol. 28, no. 5, pp. 836–840, May 1989.

[22] T. Nishinaga, K. Mochizuki, H. Yoshinaga, C. Sasaoka, and M. Washiyama, "Growth induced compositional non-uniformity in (Ga,Al)As and thermodynamical analysis," *J. Cryst. Growth*, vol. 98, nos. 1–2, pp. 98–107, Nov. 1989.

[23] R. D. Shannon, "Revised effective ionic radii and systematic studies of interatomic distances in halides and chalcogenides," *Acta Cryst*, vol. A32, no. 5, pp. 751–767, 1976.

[24] A. A. Chernov, *Modern Crystallography III. Crystal Growth*. Berlin, Germany: Springer, 1984, pp. 187–192.

[25] U. Forsberg, Ö. Danielsson, A. Henry, M. K. Linnarsson, and E. Janzén, "Aluminum doping of epitaxial silicon carbide," *J. Crsyt. Growth*, vol. 253, nos. 1–4, pp. 340–350, Jun. 2003.

[26] Y. Negoro *et al.*, "Embedded epitaxial growth of 4H-SiC on trenched substrates and PN junction characteristics," *Microelectron. Eng.*, vol. 83, no. 1, pp. 27–29, Jan. 2006.

[27] T. Kimoto, H. Nishio, W. S. Yoo, and H. Matsunami, "Growth mechanism of 6H-SiC in step-controlled epitaxy," *J. Appl. Phys.*, vol. 73, no. 2, pp. 726–732, Sep. 1997.

[28] R. K. Malhan, M. Bakowski, Y. Takeuchi, N. Sugiyama, and A. Schöner, "Design, process, and performance of all-epitaxial normally-off SiC JFETs," *Physica Status Solidi A*, vol. 206, no. 10, pp. 2308–2328, 2009.

[29] N. Nordell, S. Karlsson, and A. O. Konstantinov, "Equilibrium crystal shapes for 6H and 4H SiC grown on non-planar substrates," *Mater. Sci. Eng. B*, vols. 61–62, pp. 130–134, Jul. 1999.

[30] *Victory Process 2D—An Innovative Alternative to SUPREM-Based Simulators Ensuring Robust 3D Solutions*. Accessed: Apr. 13, 2019. [Online]. Available: https://www.silvaco.com/webinar/innovative_alternative_to_SUPREM-based_simulators_ensuring_robust_3D-solutions.html

[31] K. Mochizuki, S. Ji, R. Kosugi, Y. Yonezawa, and H. Okumura, "Effect of HCl on surface free energy of SiC during CVD trench filling," *Mater. Sci. Forum*, to be published.

[32] J. A. Burton, R. C. Prim, and W. P. Slichter, "The distribution of solute in crystals grown from the melt. Part I. Theoretical," *J. Chem. Phys.*, vol. 21, no. 11, pp. 1987–1991, Nov. 1953.

[33] A. H. Gomes de Mesquita, "Refinement of the crystal structure of SiC type 6H," *Acta Crystallographica*, vol. 23, no. 4, pp. 610–617, Oct. 1967.

[34] B. Krishnamachari, J. McLean, B. Cooper, and J. Sethna, "Gibbs-Thomson formula for small island sizes: Corrections for high vapor densities," *Phys. Rev. B, Condens. Matter*, vol. 54, no. 12, pp. 8899–8907, 1996.

[35] S. Osher and C.-W. Shu, "High order essentially nonoscillatory schemes for Hamilton–Jacobi equations," *SIAM J. Numer. Anal.*, vol. 28, no. 4, pp. 907–922, 1991.

KAZUHIRO MOCHIZUKI (M'98–SM'99) received the B.E., M.E., and Ph.D. degrees in electronic engineering from the University of Tokyo, Tokyo, Japan, in 1986, 1988, and 1995, respectively. Since 1988, he has been with Hitachi, Ltd., Tokyo. He has contributed to advances in epitaxial growth, device, and modeling technologies for II-VI, III-V, and IV-IV compound semiconductors. From 1999 to 2000, he was a Visiting Researcher with the University of California, San Diego. From 2015 to 2019, he was on loan to the National Institute of Advanced Industrial Science and Technology, Japan. He has authored or coauthored 126 research papers in international journals and conference proceedings and holds 24 U.S. patents.

RYOJI KOSUGI received the Ph.D. degree in surface science from Tohoku University, Japan, in 1999. Since 2001, he has been with the National Institute of Advanced Industrial Science and Technology, Japan. His primary interests are process development and device design toward the realization of high-performance silicon carbide (SiC) power metal–oxide–semiconductor devices. Since 2010, he has worked on research and development of the super-junction device on SiC material.

YOSHIYUKI YONEZAWA received the Ph.D. degree in SiC devices and solution growth of SiC crystal from the Tokyo Institute of Technology, Tokyo, Japan, in 2011. He was a Visiting Scholar with Stanford University, Stanford, CA, USA, from 1996 to 1999. He is currently a Team Leader of the Power Device Fundamentals Team with the Advanced Power Electronics Research Center, National Institute of Advanced Industrial Science and Technology, Tsukuba, Japan.

HAJIME OKUMURA received the B.S. and M.S. degrees in chemistry from Kyoto University and the Ph.D. degree from Osaka University, Japan. He held a research position with Electrotechnical Laboratory, MITI, including concurrent positions as a Technical Officer with Agency of Industrial Science and Technology, MITI and a General Manager with Research and Development Association for Future Electron Device. Since 2008, he has been with the Director of the Advanced Power Electronics Research Center, National Institute of Advanced Industrial Science and Technology. He has authored or coauthored over 300 scientific journal articles and holds over 30 patents.